TIGHT ROCK PERMEABILITY MEASUREMENT BY PRESSURE PULSE DECAY AND MODELING

Xiangmin Zhang[1], Christopher J. Spiers[2], Colin J. Peach[2] and Albert Hebing[1]
[1] PanTerra Geoconsultants (x.zhang@panterra.nl), [2]Utrecht University

This paper was prepared for presentation at the International Symposium of the Society of Core Analysts held in Napa Valley, California, USA, 16-19 September, 2013

ABSTRACT

Gas permeability of tight rocks of gas shale, oil shale and limestone samples was measured using a newly developed pressure pulse decay permeameter. In developing the apparatus,we adopted temperature compensated pressure transmitters, advanced data logging system and modern fitting technology. Tests can be run at confining pressures up to 10,000 psi (700 bars)and pore fluid gas pressure up to 4350 psi (300 bars). The systems were tested leakage free and the pressure decay data were further corrected with simultaneously temperature measurements to eliminate temperature effects. The permeameter has the capability of measuring range of 1mD to 1nD and with uncertainty of equivalent to permeability lower than 0.5nD. The pressure decay data were processed using similar method of Brace but taking into account the effects of the temperature and pressure dependent gas viscosity and compressibility of Nitrogen by using a Virial equation. The samples have measured permeability in the range of 0.1mD to 10 nD.

Using high pressure mercury injection (MICP) data as input and adopted integrated Darcy's and Poiseuille'sequations, the theoretical permeability of these tight rockswere calculated assuming cylindrical pore shape and compared with the measurements. Four samples were selected to perform permeability measurements with both pulse decay method and steady-state method. The measured permeability values by pulse decay are higher than those obtained by steady-state method.

INTRODUCTION

For exploration and development of unconventional resources,it is of importance to measure very low permeability (<0.1-0.01 mD) in lab for tight gas and shale gas/oil reservoir rocks. Steady state method working in this low permeability range involves measurement of very low flow ratesand high pore fluid pressure gradients across the sample. For this reason, core analysis industry uses the pressure transient pulse decay method (Jones, 1972, 1997; Bourbieet al.,1982;Ruth& Kenny, 1989; Rushing et al., 2004). The pulse decay method was originally introduced to measure the extreme low liquidpermeability in crystalline rocks for nuclear waste disposal (Brace et al., 1968; Hsieh et al., 1981; Neuzil et al., 1981). The method was later successfully used for gas permeability measurements in extreme tight rocksalt –another rock type for the nuclear waste disposal (Sutherland& Cave, 1980; Peach & Spiers, 1996). The oil and gas industry further developed the technology and applied for single phase liquid, gas permeability,two-phase relative permeability measurements (Rushing et al., 2004). Recently, the pulse decay method is extended to measure the sample porosity (Haskett

etal., 1988;Lasseux et al., 2012) and permeability measurementtaking into account the gas adsorption in samples such as shale (Cui et al., 2009).

The transient pressure pulse decay setup normally consists of an up-stream and down-stream reservoir and a sample holder. A small pressure pulse is applied in the upstream reservoir and the differential pressure allows gas flow from up-stream reservoir, through the sample and to the down-stream reservoir. The pressure changes across the sample and in the two reservoirs are recorded as a function of time.The experimental data are normally treated as gas flow non-linear equations and taking into account of the effect of the sample compressibility. Numerical and analytical methods have been used to solve the equations and to derive the gas permeability of the sample, taking into account the boundary conditions (Bourbie etal., 1982).The calculations are often simplified for some certain boundary conditions such as ignoring the sample pore volume, pore compressibility and assuming uniform gas compressibility and viscosity (Sutherland &Cave 1980; Hsieh et al., 1981; Neuzilet al., 1981). On the other hand, the developments in the mathematical and error analysis based on the differential equations enable experimental design to optimize for different samples and various purposes i. e. the up-stream and down-stream reservoir volumes, and to select experimental variables such as pulse decay pressure, gas mean pressure and duration of the experimental time etc..

The primary motivation for this study is to exchange experience in pulse decay apparatus design and to determinegas permeability of very tight rock samples.New developments in pressure transmitter, fits and data logging systems are incorporated in apparatus design, taking into account the theoretical analysis to optimizedexperimental parameters for apparatus design i. e. the reservoir volumes, temperature effects and potential leakage. We focused on the practical aspects of the experimental calibration and the procedures to facilitate the measurements of the low permeability in tight rocks. The experimental data are processed using initially the similar methods of Brace (1968) and Sutherland and Cave (1980),but taking into account the effects of the temperature and pressure dependent gas viscosity and compressibility of Nitrogen by using a Virial equation. Results of several typical tight rocks with measured permeability in the range of 113-0.01microdarcy are presented. For comparison, four samples were measured using steady-state method as well.The theoretical permeability was modeled based on the high pressure mercury injection data and compared with measured permeability results.

EXPERIMENTAL

1) The pressure pulse decay apparatus

The pulse decay apparatus, shown in Figure 1 consists of an upstream gas reservoir of volume V1, a sample holder and a downstream reservoir of volume V2. A cylindrical sample with diameter of 2.5 cm is used. The sample is placed in between two metal stems and jacketed in a rubber sleeve. The rubber sleeve is sealed against the metal stems which are graveled at endfacesto assist gas to distribute at the sample surface.The sample assembly is placed inside a hydrostatic core holder.

The volumes of the reservoirs were determined using a technique based on the PVT properties of Nitrogen and introducing an accurately known volume change to the system

whilst measuring the associated pressure changes at constant temperature. The measured reservoir volumes included dead volumes of the pressure transmitters, end-stem, connecting tubes and dead volume of relevant valves by sitting them at the same positions during a test. These were achieved by using an extra access point at the up- and down- stream respectively during the volume measurement. The access points were sealed permanently after the volume measurements. The reference known volume, which was used to measure the reservoir volumes, was pre-determined including the connection dead volume used to access the reservoir volume. To increase the measurement accuracy, the upper and down reservoir volumes were first measured separately by using dummy impermeable metal plug. The two volumes were then measured together two times by using one of the up and down stream access points while seal the other one. In upper and down streams, each has three reservoirs with various volumes. Large volumes are meant for relatively high permeability measurements. The smallest reservoir volume is used for very low permeability measurements in a relative short testing and for future development for simultaneous measurements of sample porosity during pulse decay testing (Haskett et al., 1988; Cui et al., 2009;Lasseux et al., 2012).

A differential pressure transmitter measures the pressure difference between the reservoirs, and a second transmitter measures the absolute pressure, P1, in the upstream reservoir. A third pressure transmitter is used for the measurement of the confining pressure. In PanTerra, high performance temperature compensated pressure transmitters (precision 0.01% FS) with digital RS 485 are used. The pressure transmitter consists of a pressure sensor, a temperature sensor and a microprocessor. A mathematical model is used to derive the precise pressure value (P) from signals measured by pressure sensor (S) and temperature sensor (T). The microprocessor in the transmitter calculatesthe pressure using a polynomial equation. Each pressure transmitter outputs calculated pressure measurements as well as the simultaneous temperature measurements. Commercial software from the transmitter supplier is used to log experimental data.

Hydrostatic confining pressure can be applied upto 10,000 psi (700 bars) and gas pore pressure upto 4350 psi (300 bars). The apparatus is installed in an air-conditioned room and temperature is controlled within ±0.5 °C. A vacuum pump is installed to facilitate the purge of the system and sample during preparation.Nitrogen is supplied from a gas bottle and its desired pressure for a test is regulated by a pressure regulator.

2) The testing procedure and data

A test starts with a test design for selecting the right reservoir volumes based on the sample porosity. After loaded and desired confining pressure applied, a vacuum purge of the system and sample is carried out before filling the system with Nitrogen gas. The system is then re-purged and filled once more. This ensures the system and sample contain only Nitrogen gas.The sample and both selected up- and down-stream reservoirs are then filled simultaneously with Nitrogen gas at desired pressure. Pressure equilibrium takes different times depending on the sample property. The upper- and down-stream reservoirs are then separated each other. A pressure pulse (20-50 psi above the equilibrium pressure) is generated and applied on the upper reservoir which enables gas flow from the upstream reservoir across the sample and into the downstream reservoir.

The pressure at upper stream reservoir will then decrease, while in the down-stream pressure will build up until new pressure equilibrium reached. Figure 3 shows an example of the pressure pattern in the upper and down-stream reservoirs. After test finished, data are exported into Excel for further processing.

Several blank runs were carried out by using an impermeable metal dummy sample. Experimental variables were set at various typical testing conditions with respect to the confining pressures, up- and down- reservoir pressures, differential pressures and temperature, but with prolonged time. The pressure return tests were carried out by applied a fixed pressure at both reservoirs for several days. The pressure measurements were compared when the exact sample temperature return the same in an interval of 24 hours. These data were used to check the potential leakage at upper and down-stream reservoir respectively.The potential leakage of our system is equivalent tosample permeability less than 0.5nD. The influence of room temperature fluctuations on the differential pressure are studied in the blank run with deliberately setting larger temperature changes than in a real test run. The results are shown in Figure 2 and are applied to all tests for temperature correction by adjusting measured differential pressure to a reference temperature (mean experimental temperature=21 °C).

3**) Data processing and permeability calculation**

After exporting the raw data into an excel file, all the pressure data are corrected for temperature effects as described in above. The apparent gas permeabilitywas then calculated based on the method original proposed by Brace et al. (1968). The pulse is a small step change of differential pore fluid pressure imposed between two reservoirs connected at the ends of the sample. When a pressure pulse ΔP_0 is applied, the differential pressure $\Delta P(t)$ decays exponentially as a function of time*t*(Sutherlandand Cave, 1980; Peach and Spiers, 1996)

$$\Delta P(t) = \Delta P_0 \, e^{-mt} \qquad (1)$$

Where, *t* is testing time and *m*is a decay time constant. Plotting the decay curve in terms of $ln[\Delta P(t)]$ vs. time *t* yields a straight line having a slope *m* (Figure 3), and the permeability *k* can be determined (Sutherland and Cave, 1980) by

$$k = m\mu\beta(L/A) \times [V1\ V2/(V1 + V2)] \qquad (2)$$

where

V_1,$V_2$are the upstream and downstream reservoir volumes

L = length of the sample,

A = cross-sectional area of the sample,

μ = Nitrogen viscosity at temperature and mean pore pressure (Lemmon& Jacobsen2004), and

$\beta$is the compressibility of Nitrogen which is calculated using Virial function for compressibility factor

$$Z = PVm/RT = 1 + B/Vm + C/V2m + ... \qquad (3)$$

where*R* is the gas constant.*B,C,...*, are the second, third,...virial coefficients which for a given substance are functions of temperature only.The second virial coefficient *B* of a gas can be fittedby an equation of the form:

$$B = a - b\ exp\{c(K/T)\} \quad (4)$$

a=185.4;*b*=141.8;*c*=88.7 for Nitrogen (Span et al. 2000). The third virial coefficient and forward can be neglected.

In calculation permeability of samples with high adsorption capacity such as in certain types of gas shale, Cui et al. (2009) useda similar equation as above equation (2) but with an extra item of adsorption factor $1/f_1$. The adsorption factor is a function of adsorption volume compared to the sample porosity (Cui et al., 2009). In our calculation, the effect of adsorption is neglected.

EXPERIMENTAL RESULTS AND MODELING

1) Permeability results by pulse decay

The sample and permeability measurement results are listed in Table 1. Thirty two measurements were carried out on 21 samples of tight limestone, gas shale, oil shale and tight siltstone samples with 1 inch diameter. Porosity values, which were separately measured either by Helium pycnometryor MICP method, were in the range of 0.2-17.6%. The confining pressureswere from 800 to 3,200 psi. The initial equilibrium pore pressureswere in the range of 225 to 950 psi. Initial pressure pulse in the range of 50-20 psig was applied. Each individual test run lasted from hours to 3 days. The measured gas permeability is in the range of 0.01 to 113 microdarcy.

The limestone sample of LS10 was tested with 6 step mean pore pressures to obtain the Klinkenberg gas permeability and the results are shown in Figure 6 and in Table 1. The apparent gas permeability at low mean pore pressure of 19 psig is 48.98microdarcy and 13.74 at 103 psi. The Klinkenberg permeability extrapolated to infinite high mean pore pressure is 6.03 microdarcy as shown in Figure 6.

The other limestone samples (LS1-LS9) were measured at mean pore pressure of 225 psi. The helium porosity of these samplesare from 0.2-7.65%. The measured permeability are in the range of 0.98-4.73 microdarcy.

The BS1-BS4 samples are black shale from a gas reservoir. The measured permeability is in the range of 0.08-12.31 microdarcy. Note for sample BS-1, the confining pressure increased from 1,200 psi to 2,400 psi this resulted in permeability decrease from 12.31 to 4.31, a factor of 3.

The oil shale samples OSH and OSV were drilled from a hand specimen (Figure 5) in the direction of horizontal and vertical direction respectively. This is a sample with original oil stained in the upper and low part of the specimen. However, in the middle of the specimen, it is lack of oil stain, apparently seen from Figure 5. The distribution of stained oil indicates permeability contrast in the horizontal and vertical directions. The permeability were measured as received, meaning no lab cleaning for them. The vertical permeability is as low as 0,01microdarcy(OSV-1, & OSV-2). The horizontal gas permeability decreases from 8.45 to 4.5 microdarcyfrom confining pressure 1,200 psi to 3,200 psi.

The siltstone sample (SS-1 to SS-4 and SSr) are homogenous samples in the plug scale. Their permeability is in the range of 2.8 to 113 microdarcy.

2) Permeability measurement by steady state method

For comparison, four samples (OSH-3-SS; OSV-1-SS; SS1-SS and SSr-SS) with various pulse decay permeability were selected to perform permeability measurements using steady state method. This was achieved by using an extra low flow rate mass flow meter and high gas pressures. The results are listed in Table 1.

3) Permeability modeling based on MICP

Numerous theoretical attempts have been made to relate the permeability *k* to other more easily measurable properties such as porosity and porediameters. One such approach (Purcell, 1949) models the flow of fluids across straightcylindrical pore by combining Darcy's and Poiseuille's laws to obtain

$$k_i = \frac{\phi_i d_i^2}{32} \qquad (5)$$

Whereϕ is porosity and *d* is the mean pore diameter. Correction for non-uniform pore characteristics leads to an expressionof the general form of

$$k = \frac{\phi d^2}{16\tau} \qquad (6)$$

whereτ can be taken to represent the effective tortuosity of the pores. If the poresare assumed to be straight cylindrical capillaries then τ=2.

At a mercury displacement pressure, P_i, the pore diameter d, which can be penetrated by mercury is given by:

$$d_i = \frac{4\sigma \cos\theta\, c}{P_i} \qquad (7)$$

where:

r = pore throat diameter, μm

σ = interfacial tension between air and mercury, dynes/cm (480)

θ = contact angle between air and mercury, degrees (140)

P_i = capillary pressure, psia

C = conversion constant (0.145)

Assuming the rock sample pores are of a bundle of cylindrical tube, the total permeability of a rock sample can be obtained by integrating the pore throat size distribution curves derived MICP capillary curve. For practical calculation from a MICP data set normally provided by a core analysis service lab, the following accumulation equation can be used

$$k = \sum_{i=1}^{j} \frac{\phi_i d_i^2}{32} \qquad (8)$$

Where ϕ_i is the ratio of mercury injection volume at injection pressure Pi to the sample bulk volume and $d_i$is given in equation (7).With knowledge of rock tortuosity from formation resistivity factor measurement, equation (6) can be used for the integration. Such works have been done recently on high permeability rocks by Ruth et al. (2012).

The MICP capillary pressure curves are shown in Figure 4. The derived pore throat size distributions are shown in the rest diagrams of Figure 4 and are grouped in three for clarity. It is clear that the pores size are in the range of <100 nm.

DISCUSSION

The uncertainties of the measurements by pressure pulsed decay, the comparison with steady state permeability and model results based on MICP are discussed below.

1)**Uncertainties of permeability results**

The quality of permeability measurement using pressure transient pulse decay method depends on permeameter design, individual testing design & procedure, the calculation method, as well as the sample property. All calculation methods need simplified assumptions to obtain an analytical solution of the non-linear flow equation (Brace, 1968; Bourbie et al, 1982; Jones, 1972; Lasseux et al., 2012). The validity of these assumptions depends on the permeameter design, test design and procedures together with the sample properties. More specific, the following factors influence the accuracy of permeability measurement in this study: the gas reservoir volumes, potential leakage, temperature effects on measured pressures, Klinkenberg effect, sample pore volume (porosity) and potential sorption capacity of the sample etc.

The equipment calibration and validation stages are key steps to evaluate and control the uncertainties inherent to any experimental equipment. During this work this has been achieved by using various reservoir volumes for an individual test design according to a sample property – mainly the porosity. Series of blank runs with impermeable samples allow us to estimate the potential leakage of the system. The blank runs enable us to derive an empirical correction function for temperature effects, which is very close to the theoretical prediction. The pressure return test and the close match of temperature effects on measured pressure and theoretically calculated values confirmed that the system is well sealed and any potential leakage contributions are less than 0.5nD.

The large error origin for our permeability measurements is pore volumes. Because the apparatus is designed for tight rocks, in our calculation (Equation 2 & 3) the porosity is neglected. Rough estimation by adding half sample pore volume to up and down reservoir volumes (medium size reservoirs) for high porosity samples such as LS9, LS10, SS1 and SSr show that 2-5% error may occur. Even larger error may occur if smaller reservoir were used. Klinkenbergeffects are big in low permeability samples as shown in LS10 especially when low gas mean pore pressure applied. It is hence recommended to either fully determine the Klinkenberg effect or carry out a single test at elevated mean pore pressure (Jones, 1972), i. e. at 2MPa (20bar) or higher.

Another potential error for permeability measurements is the adsorption of gas during the transient pulse decay. Cui et al. (2009) estimated that gas permeability can have 10% error for high adsorption gas shale. More work would need to be done on that subject.

2) Comparison of measured gas permeability with modeled based on MICP data

Our experimental results show that pulse decay permeability is consistently higher than the steady state permeability (Figure 7), even compared at similar confining pressures and mean pore gas pressure. This result is in good agreement with Kamath et al. (1992), Rushing et al., (2004) and Carles et al., (2007).The calculated permeability results based on the high pressure mercury injection data are in the same order of magnitude as the pulse decay measured permeability. The Pulse decay measured permeability is generally higher than the MICP permeability. The first likely reason is that in modeling we assume the pores in the tight rocks have a cylindrical geometry. It is known that the pore structures and geometry are complex in tight rocks and can differ significantly from cylindrical shapes. More suitable geometrical models of pore in certain rock types are needed. The second reason is that the MICP modeling did not take into account the directional heterogeneity of the rock sample such as in laminated shale. More work would need to be carried out in tight rocks such as in shale to resolve this.

CONCLUSIONS

Pressure pulse decay experiments are suitable for determining permeability in core samples from very tight formations such as in gas shale, oil shale and tight limestone etc..Proper design and careful calibration of the apparatus, individual test design can eliminate uncertainties and increase the measurement accuracy. Modeled permeability based on pore throat size distributions in tight rock can generally agree in the same order of magnitude. Geometrical models of pore in certain rock types are needed.

ACKNOWLEDGEMENTS

Sample of oil shale was kindly provided by Mr. Eddy Anderson from NAM. Technical support from Mr. Cor Laffra,Mr. James Ryan,andMr. Sander Huisman are acknowledged.The authors would also like to thank Dr. Patrick Egermann and Dr. Josephina Schembre for reviewing the paper.

REFERENCES

1. Brace, W. F., Walsh, J. B. and Frangos, W. T., 1968, Permeability of granite under high pressure, *Journal of Geophysical Research73*, 2225-2236, 10.1029/JB073i006p02225.
2. Bourbie, Thierry Walls, Joel, 1982, Pulse Decay Permeability: Analytical Solution and Experimental,*SPE Journal 22*, 5, P719-721, 10.2118/9744-PA.
3. Carles, P., Egermann, P., Lenormand, R., Lombard, J. M., 2007, Low permeability measurements using steady-state and transient methods, *International Symposium of theSociety of Core Analysts*,SCA2007-07.
4. Cui, X. Bustin, A. M.and Bustin, R. M., 2009, Measurements of gas permeability and diffusivity of tight reservoir rocks: different approaches and their applications, *Geofluids*, 208-223, 10.1111/j.1468-8123.2009.00244.x
5. Haskett, S. E., Narahara, G. M., and Holditch, S. A., 1988, A method for simultaneous determination of permeability and porosity in low permeability cores, *SPE Formation Evaluation*, 651-658.

6. Hsieh, P.A., Tracy, J.V., Neuzil, C.E., Bredehoeft, J.D. and Silliman, S.E., 1981. A transient laboratory method for determining the hydraulic properties of 'tight' rocks - I. Theory. *Int. J. Rock Mech. Min. Sci. and Geomech. Abstracts18,* pp. 245-252.
7. Jones, S. C., 1972, A rapid accurate unsteady-state Klinkenbergpermeameter, *Soc. Pet. Eng. J., 12,* (5), 383–397.
8. Jones, S.C., 1997,A Technique for Faster Pulse-Decay Permeability Measurements in Tight Rocks, *Journal SPE Formation Evaluation12,* 19-26, 10.2118/28450-PA.
9. Lasseux, D., Jannot, Y, Profice. S., Mathieu Mallet, M., and Hamon, G., 2012,The "step decay": A new transient method for the simultaneous determination of intrinsic permeability, klinkenberg coefficient and porosity on very tight rocks, *International Symposium of the Society of Core Analysts*, SCA2012-25.
10. Lemmon, E. W. and Jacobsen, R. T., 2004, Viscosity and Thermal Conductivity Equations for Nitrogen, Oxygen, Argon, and Air, *International Journal of Thermophysics 25*, 21-69.
11. Neuzil, C.E., Cooley, C., Silliman, S.E., Bredehoeft, J.D. and Hsieh, P.A., 1981. A transient laboratory method for determining the hydraulic properties of 'tight' rocks II.-Application. *Int. J. Rock Mech. Min. Sci. and Geomech. Abstr. 18*, pp. 253-258.
12. Peach, C. J and Spiers, C. J.,1996, Influence of crystal plastic deformation on dilatancy and permeability development in synthetic salt rock, *Tectonophysics 256*, 101-128.
13. Purcell, W.R., 1949, Capillary Pressures – Their Measurement using Mercury and the Calculation of Permeability Therefrom, *AIME Transactions*, (TP 2544), Vol. 186, pp. 39-48.
14. Rushing, J., Newsham, K., Lasswell, P., Cox, J., Blasingame, T., 2004, Klinkenberg-Corrected Permeability Measurements in Tight Gas Sands: Steady-State Versus Unsteady-State Techniques, *SPE Annual Technical Conference and Exhibition*, SPE 89867.
15. Ruth, D. W., and J. Kenny, 1989,The unsteady-state gas permeameter, *J. Can. Pet. Technol, 28*, 67–72.
16. Ruth,D. C. Lindsay, and M. Allen, 2012, Combining Electrical Measurements and Mercury Porosimetry to Predict Permeability, *International Symposium of the Society of Core Analysts,* SCA2012-28
17. Span, R., Lemmon, E. W, Jacobsen, R. T., Wagner, W. and Yokozeki, A., 2000, A reference equation of state for the thermodynamic properties of Nitrogen for temperatures from 63.151 to 1000 K and pressures to 2200 MPa, *J. Phys. Chem. Ref. Data 29*, No.6, 2000, 1361-1433.
18. Sutherland, H.J. and Cave, S.P., 1980. Argon gas permeability of New Mexico rock salt under hydrostatic compression. *Int. J. Rock Mech. Min. Sci. and Geomech. Abstr.17,* pp. 281-288.

Table 1: Results of permeability measurements by pressure pulse decay and modelled by MICP.

Test ID	Rock Type	Length (cm)	Diam (cm)	Confining Pressure (psig)	Equilibrium Pore Pressure (psig)	Porosity (%)	Pulse Decay Permeability (micro-Darcy)	MICP Permeability (micro-Darcy)
LS1	Limestone	2.42	2.52	800	225	3.1	1.77	1.84
LS2	Limestone	3.99	2.54	800	225	3.7	3.12	-
LS3	Limestone	2.65	2.53	800	225	2.4	4.73	-
LS4	Limestone	2.90	2.55	800	225	1.0	0.98	0.32
LS5	Limestone	3.99	2.55	800	225	0.2	2.22	-
LS6	Limestone	3.72	2.43	800	225	1.0	3.65	-
LS7	Limestone	2.03	2.49	800	225	3.3	3.76	-
LS8	Limestone	4.04	2.53	800	225	5.5	2.88	-
LS9	Limestone	4.05	2.53	800	225	7.6	4.15	2.74
LS10-1	Limestone	4.05	2.53	375	19	11.0	48.98	-
LS10-2	Limestone	4.05	2.53	375	46	11.0	23.29	-
LS10-3	Limestone	4.05	2.53	375	68	11.0	17.72	-
LS10-4	Limestone	4.05	2.53	375	84	11.0	15.57	-
LS10-5	Limestone	4.05	2.53	375	90	11.0	14.85	-
LS10-6	Limestone	4.05	2.53	375	103	11.0	13.74	-
BS1-1	Shale	1.82	2.51	1200	250	-	12.31	-
BS1-2	Shale	1.82	2.51	2400	250	-	3.17	-
BS2	Shale	1.93	2.52	1200	250	1.0	0.44	0.31
BS3	Shale	3.99	2.52	1200	250	0.2	0.11	0.01
BS4	Shale	3.99	2.52	1200	250	0.3	0.08	0.03
OSH-1	(oil)Shale	3.12	2.52	1200	250	-	8.49	-
OSH-2	(oil)Shale	3.12	2.52	2400	250	-	5.54	-
OSH-3	(oil)Shale	3.12	2.52	3200	250	-	4.05	-
OSH-3-SS*	(oil)Shale	3.12	2.52	3200	Pin=500	-	1.96 (SS)	-
OSV-1	(oil)Shale	3.44	2.53	3200	250, 500	-	0.02	-
OSV-1-SS*	(oil)Shale	3.44	2.53	3200	Pin=1500		0.01 (SS)	-
OSV-2	(oil)Shale	3.44	2.53	2400	300, 950	-	0.01	-
SS1	Siltstone	2.52	2.52	2400	375	12.8	16.18	11.00
SS1-SS*	Siltstone	2.52	2.52	2400	Pin=500	12.8	14 (SS)	11.00
SS2	Siltstone	2.51	2.52	2400	300	-	2.84	1.80
SS3	Siltstone	3.45	2.49	2400	300	-	8.49	-
SS4	Siltstone	4,04	2.53	2400	300	3.7	20.07	32.40
SSr	Sandstone	2.54	2.54	2400	300	17.6	113	33.15
SSr-SS*	Sandstone	2.54	2.54	2400	Pin=150	17.6	97 (SS)	33.15
BR-1	Metal	2.54	2.54	3200	300; 600; 900	0.0	0.00	-

*Measured with steady-state method.

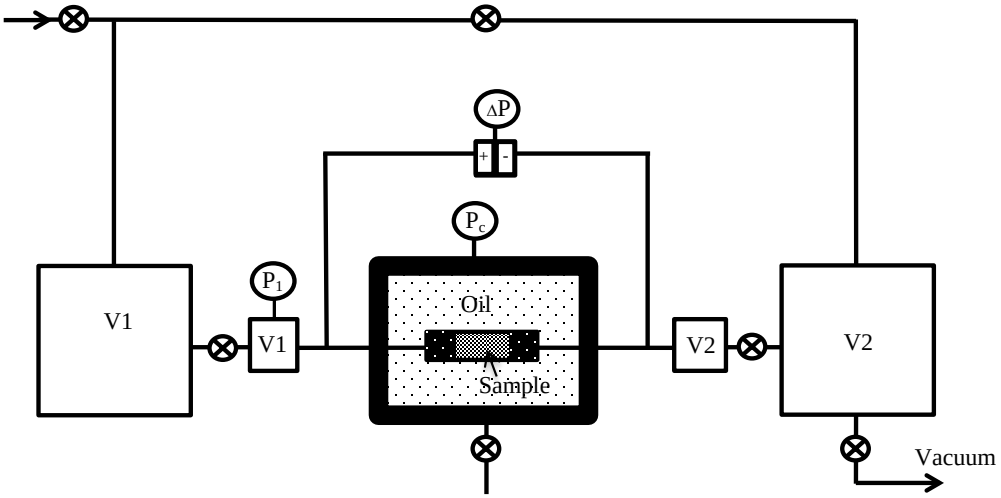

Figure 1. Schematic diagram of the setup for pulse decay permeametry.

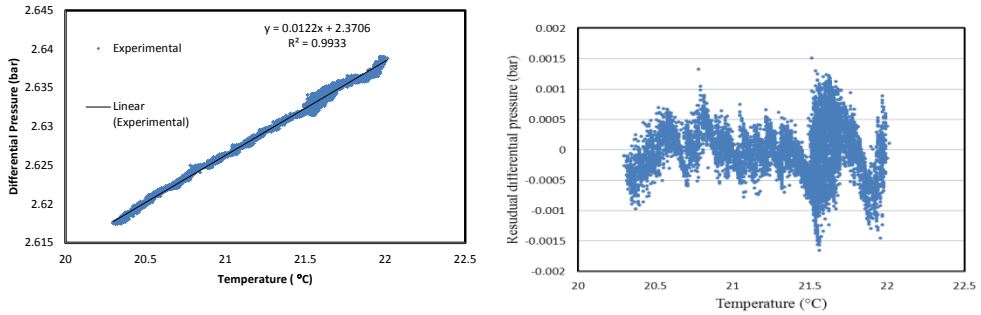

Figure 2. Temperature correction for differential pressure. Test was run with impermeable dummy sample (no flow). Left: Experimetally measured temperature effect on differential pressure; Right: Residual differential pressure corrected for temperature effect on the same data(reference to 21 °C).

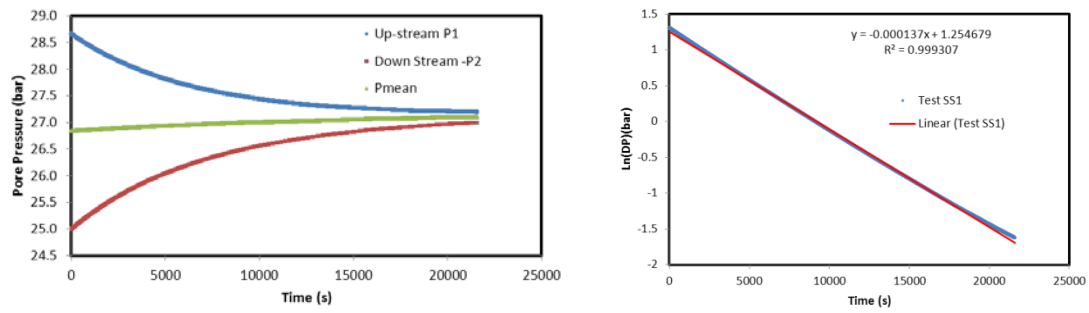

Figure 3. Pressure pulse decay for sample SS1. Left: Pressures in up- and down- stream reservoirs and mean pore pressure. Right. Differential pressure decay.

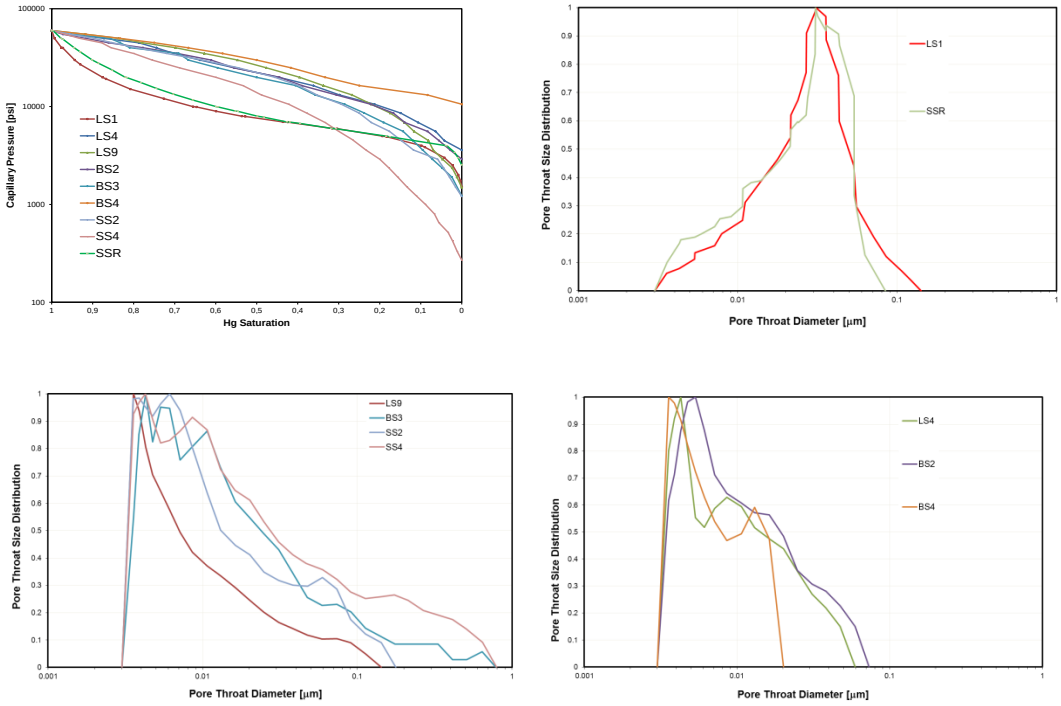

Figure 4. High pressure mercury injection (MICP) capillary curves for 9 samples and the derived pore throat size distributions. Pore throat size distributions are used to calculate theoretical permeability.

Figure 5. Photograph of hand specimen of oil shale. Note the oil stained parts at top and bottom. Middle part is oil free. Samples OSH and OSV are plugged in the horizontal and vertical direction respectively.

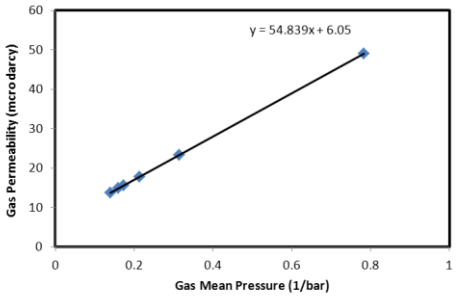

Figure 6. Klinkenberg permeability of sample LS-10.

Figure 7. Comprison of permeabilty measured using pulse decay and steady state method for four samples.